Imaging Transmission Line Impedance Profiles using Passband Signals and Adaptive Sequence Design

Jehiel Santos, Wenjie Wang, Ross Murch

Department of Electronic and Computer Engineering
The Hong Kong University of Science and Technology
jdsantos@connect.ust.hk, wwangbk@connect.ust.hk, eermurch@ust.hk

***Abstract*—The problem of imaging transmission line impedance profiles for fault location is considered. The approach utilized makes use of a novel adaptive probing sequence. The sequence is constrained to be unimodular and trained to obtain the minimized mean square error between the channel estimate and the true channel response. To achieve a practical approach for the reconstruction process, bandlimited passband signals are also considered so that the method can be applied to real systems with a limited bandwidth. This imposes a challenge as only bandlimited information is available for profile reconstruction. Therefore a technique for exact reconstruction with bandlimited signals is also proposed. Results are provided and it is demonstrated that the use of bandlimited passband signals performs well for transmission line impedance profile reconstruction under various conditions.**

***Index Terms*—transmission lines, impedance profiling, adaptive signal processing, digital signal processing, VLSI, PAPR**

I. Introduction

FAULT detection and fault location in electrical networks has become more important as systems, VLSI circuits and infrastructures become more dependent on wired and optical networks [1], [2]. For example in the fabrication process of VLSI circuits, transmission line defects can occur, and these need to be identified [3]–[5]. To detect sharp discontinuities or hard faults along transmission lines, reflectometry-based techniques are widely used [1]. Methods have also been developed for detecting small variations in impedance and these are often classified as soft faults, which are smooth and localized inhomogeneities in the transmission lines [2]. These are early indications that a cable is starting to lose its reliability or that the VLSI defects are more subtle and might lead to intricate problems if left undetected. While reflectometry is known to effectively detect hard faults, it is inadequate for identifying weak faults [6]. Therefore, alternative methods have been proposed for the detection of soft faults [2], [7], [8].

In this paper, we make contributions to the reconstruction of impedance profiles in transmission lines for the detection of both hard and soft faults. Our reconstruction approach is formulated in the practical context of bandlimited passband signals that are modulated onto a carrier. This allows systems that only operate in specific frequency bands and bandwidths to utilize the technique to perform self diagnosis of faults. Furthermore, unimodular signals are considered so that the peak-to-average ratio (PAPR) characteristics of the signals are close to unity for supporting efficient power amplifier design [9]. The method utilizes a novel adaptive sequence approach in determining the probing signals. It involves updating a short probing sequence (3 symbols) based on the received reflected signals to achieve a minimized mean square error between the channel estimate and true channel response. To meet the challenge of the limited information obtained about the impedance profile, due to the bandlimited passband signals utilized, a novel method based on sample accumulation is proposed to obtain exact reconstruction of certain impedance profile types.

Impedance profiling can be considered a type of one-dimensional imaging and shares some characteristics with higher-dimensional imaging such as tomography, ultrasonic and medical imaging, remote sensing, and radar [10]–[13]. Generally, imaging can be formulated as an inverse scattering problem whereby a target is probed by transmit pulses so that the target can be reconstructed based on the measured reflected signals. Research on one-dimensional inverse scattering for detecting soft faults, [2], [7] has experimentally demonstrated that accurate reconstruction of transmission line impedance profiles is possible. The approach in [7] provides intuitive insight between the empirical process of reflectometry and the exact methods based on Zakharov-Shabat (ZS) equations [14]. We use that approach [7] in the results presented here.

The remainder of the paper is organized as follows. In Section II, we describe the transmission line model. In Section III, we introduce the formulation for the adaptive sequence design. In Section IV, numerical simulations are provided followed by conclusions in Section V.

II. Transmission Line Model

To consider defects in the transmission line, we use $Z(z)$ to represent the distributed characteristic impedance, where z is the longitudinal axis of the line. The transmission line length is denoted as a and it is excited by a voltage source which

has an angular frequency ω at the left end and matched to a load at the right end. The impedance is then defined as

$$Z(z) = \sqrt{\frac{L(z)}{C(z)}}, \tag{1}$$

where $L(z)$ and $C(z)$ are the inductance and capacitance at any point z. The wave speed $c(z)$ is expressed as $c(z) = 1/\sqrt{L(z)C(z)}$. We also define the wavenumber as $k = \omega/c(0)$ and the refractive index as $v(z) = c(0)/c(z)$. A time harmonic variation of $e^{-j\omega t}$ is assumed such that the total voltage and current at any point z can be written as $V(z,k)$ and $I(z,k)$. Assuming that a fault is present in the line, an incident voltage $V_{\text{inc}}(z,k)$ will cause a scattered voltage $V_{\text{s}}(z,k)$ to exist. The return loss or reflection coefficient $S_{11}(k)$ is then obtained by taking the ratio of the measured data set at the source $V_{\text{s}}(0,k)$ and the given excitation $V_{\text{inc}}(0,k)$ such that

$$S_{11}(k) = \frac{V_{\text{s}}(0,k)}{V_{\text{inc}}(0,k)}. \tag{2}$$

This $S_{11}(k)$ parameter can be measured in practice using a vector network analyzer (VNA). The Liouville transform is invoked to convert the spatial length z into the electrical length x. This is performed to remove the effect of varying wave propagation speed along the line by evaluating

$$x(z) = \int_0^z v(s)ds. \tag{3}$$

The total electrical length becomes $b = x(a)$ and $x = [0, b]$.

In this work, the excitation or probing signal $V_{\text{inc}}(0,k)$ is composed of pulses or a sequence that will be modulated by a carrier frequency for practical purposes. This sequence is passed through an adaptive sequence algorithm, as described in the next section, to obtain the optimum sequence and the optimum estimate of the channel. At the end of the iterative process, the optimum channel estimate is used to reconstruct the impedance profile using the expression [7]

$$Z(x) = Z(0)\exp\left(\int_0^{2x} 2\mathcal{F}^{-1}[S_{11}(k)](s)ds\right). \tag{4}$$

This expression is based on the Born approximation and performs well for a wide range of impedance variations [7]. The final step is to transform the electrical coordinate x back to the spatial coordinate z using

$$z(x) = \int_0^x \frac{ds}{v(s)}. \tag{5}$$

III. Channel Model and Sequence Design

The system for imaging the transmission line impedance profile is shown in Fig. 1. The probing signals $\text{Re}\{u(t_0)\}$ and $\text{Im}\{u(t_0)\}$ are passed through a raised-cosine pulse shaping filter (to form the bandlimited response) and modulated at a carrier frequency $\omega_c = 2\pi f_c$. These signals are passed through the transmission line whose characteristics are denoted by $h(t)$ in Fig. 1. The impulse response $h(t)$ is the temporal Fourier Transform of the reflectivity $S_{11}(k)$ in eq. (2). Once the signal passes through the channel at the receiving side, the signal is demodulated and passed through a matched filter. Finally, the signal is downsampled.

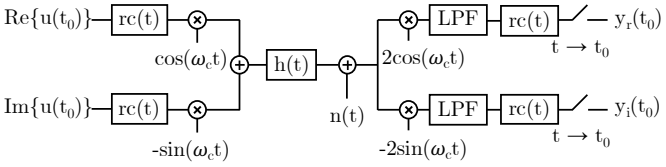

Fig. 1: System Set-up

The challenge of the design of the system shown in Fig. 1 is the design of the input signals so that the resulting output signals can be processed to determine an estimate of $h(t)$ and subsequently utilized in eq. (4) for reconstruction. In this paper, we examine the design of the excitation signal realized by a unimodular sequence $u(t)$ (for good PAPR characteristics) with sequence length N. In practice $u(t)$ is the voltage excitation $V_{\text{inc}}(0,k)$. This sequence $[u_1 u_2 \cdots u_N]$ is iteratively updated during the estimation process to increase the accuracy of the channel estimate by adaptation based on the resulting received output at each iteration. That is, we send a sequence of length N, use the resulting received output to form another sequence of length N that can produce a better estimate of the channel and so on. The total number of iterations or rounds is denoted as l. We use the PAPR-constrained adaptive sequence design based on approach proposed from [9].

The sampled channel impulse response $h(t_0)$ with length K is estimated from the information provided by the received sequence $y(t_0)$ obtained by taking the discrete convolution of channel and input signal. A noise vector $n(t_0)$ is then added denoted by $[n_1 n_2 \cdots n_{N+K-1}]$. In matrix form, this operation can be written as

$$\mathbf{y} = \begin{bmatrix} y_1 \\ \vdots \\ y_{N+K-1} \end{bmatrix} = \begin{bmatrix} u_1 & & \mathbf{0} \\ \vdots & \ddots & u_1 \\ u_N & \ddots & \vdots \\ \mathbf{0} & & u_N \end{bmatrix} \begin{bmatrix} h_1 \\ \vdots \\ h_K \end{bmatrix} + \begin{bmatrix} n_1 \\ \vdots \\ n_{N+K-1} \end{bmatrix} \tag{6}$$

which can be further simplified by defining $\mathbf{S_u} = \mathcal{T}(\mathbf{u})$, with size $(N+K-1) \times K$, as a Toeplitz convolution matrix of the input sequence $\mathbf{u}$ to give

$$\mathbf{y} = \mathbf{S_u}\mathbf{h} + \mathbf{n}. \tag{7}$$

Given the observation $\mathbf{y}$, a channel estimate $\hat{\mathbf{h}}$ is obtained by using a nested loop based from mathematical formulation that uses majorization-minimization framework [9]. It begins with an initial randomly selected unimodular sequence that updates until the mean square error function is minimized. Then, a channel estimate is obtained when the converged sequence is transmitted to the channel. After the number of training rounds l is complete, the final channel estimate is retrieved for the reconstruction of the impedance profile. In total, $N \times l$ samples will have been transmitted in the process. It should also be noted that using a short ($N = 3$) sequence length N trained for several rounds, say $l = 256$, usually obtains greater accuracy than using a long sequence trained for less rounds, say $N = 768$ transmitted once ($l = 1$). Hence for this procedure, shorter sequence N with more training rounds l is selected.

IV. Exact Reconstruction using Accumulation

The problem with the bandlimited passband system approach shown in Fig. 1 is that only information about $h(t)$ is known over a limited band. For the proper reconstruction of the impedance profile using eq. (4) we need a wideband estimate of $S_{11}(k)$ (or equivalently $h(t)$ in time-domain). However we only have a bandlimited passband estimate. To resolve this, steps can be added prior to downsampling at the receiving end using sample accumulation.

The objective of the sample accumulation method is to recover the received signal similar to when wideband baseband pulses are transmitted. This is accomplished by realizing that for some fault profile types, such as rectangular profiles, the channel frequency response is periodic and hence, obtaining a portion of the channel is sufficient to estimate the entire channel response. This can be performed by first equalizing out the effect of the RC pulse shaping filters within the bandwidth of the transmit signal. Then, we undo the spreading effect of the low pass filters by accumulating the samples within a range defined by an oversampling factor, γ. This factor is obtained by taking the ratio of the sampling frequency of the carrier and the actual carrier frequency. The details of the process are shown in Algorithm 1. The intuition behind this is to combine the energy of the samples every γ to the point where the maximum sample value occurs. We identify the boundary of the accumulation range to avoid having multiple accumulation points in the same range. This is done by defining position p as the initial point and k as the location of the maximum value from p to γ. Finally, a phase compensation $e^{j\omega_c t}$ is introduced to shift the received signal back to its baseband equivalent.

Algorithm 1 Sample Accumulation

1: Initially set $y(t) = \mathbf{0}$, $\alpha = 1$, $p = 2$
2: **repeat**
3: $k =$ position of $\max\{y(t_i)\}$ within $[p, \alpha\gamma + 1]$
4: Accumulate $y(t_{p+k-1}) = \sum_{i=p}^{\alpha\gamma+2} y(t_i)$
5: $p =$ position of $\max\left\{\gamma(\alpha - 1) + k + \frac{\gamma}{2}, \alpha\gamma + 2\right\}$
6: $\alpha \leftarrow \alpha + 1$
7: **until** $\alpha = N + K - 1$

V. Numerical Simulations

To demonstrate the approach, we employ numerical simulations of bandlimited baseband and passband signals for channel estimation and profile reconstruction characterized by a rectangular impedance profile $Z(z)$. Standard reflection and transmission transformation formulas [15] were used to obtain the measurement data set of the inverse problems in determining the reflection coefficients at the left end. Since the impedance profile is continuous along the transmission line, the transformation formulas were discretized and concatenated over each interval.

For our numerical simulations, a step size of $\Delta z = 0.0001$ m is selected. We assume that the capacitance is fixed at $C = 0.01$ nF/m and the characteristic impedance is $Z(0) = 50\ \Omega$. Then, the resulting inductance and wave speed are $L(0) = 250$ nH/m and $c(0) = 2 \times 10^8$ m/s respectively. Since the capacitance is assumed to be constant along the line, the electrical length x can be converted to spatial coordinate z using the reconstructed $Z(x)$.

A sequence length $N = 3$ is sent $l = 2^8$ rounds in the channel. Each symbol is separated by $T_{sy} = 0.5$ ns resulting in $f_{sy} = 2$ GHz bandwidth. This is modulated by $f_c = 4$ GHz carrier frequency, which is discretized and sampled at a rate of $f_{cs} = 20$ GHz. The minimum oversampling factor, γ is obtained by taking the ratio of f_{cs} and f_c. In this simulation, we use γ equal to 10. The factor γ is considered for the downsampled signals and continuous time passband signals. Thus, the reflection coefficient for the baseband case is observed over the frequency range of 0 to 1 GHz, while the passband case is from 3 to 5 GHz. Later, the effect of noise is also considered which satisfies $\mathcal{CN}(0, \mathbf{W})$, where $\mathbf{W}$ is the noise variance.

We consider a rectangular impedance profile in which the peak impedance deviation is selected to be 5% of $Z(0)$, which in this case is 2.5Ω. This ensures that the Born approximation will perform well since $Z(z)$ is close to $Z(0)$. This isolates the performance of the approximate reconstruction process eq. (4) for better evaluation of the adaptive sequence design. The performance of the algorithm and reconstruction is measured by the average absolute relative error over z and expressed by

$$e_{\text{rel}} = \frac{1}{z}\int_0^z \left|\frac{Z_{\text{Born}}(l) - Z_{\text{exact}}(l)}{Z_{\text{exact}}(l)}\right| dl. \tag{8}$$

This metric of error provides a direct assessment of the reconstructed profile in comparison to the exact profile to allow comparison of different transmit signals and its respective reconstruction performance.

A. Baseband Set-up

This set-up demonstrates the reconstruction performance of the adaptive sequence design in noiseless condition using wideband baseband pulses. Specifically, we consider a 2 m transmission line and the results are shown in Fig. 2. It can be seen that the designed sequence is effective in recovering the impedance profile $Z(z)$ with varying fault lengths, each with a relative error e_{rel} of $2.7\%, 2.8\%, 2.9\%$, and 5.4% for Fig. 2 (a)-(d) respectively. These results also serve as a reference for the simulations of the passband case.

We also compare the performance of the unimodular sequence to a single impulse signal approach [7]. In order to make the measurements comparable, the impulse signal is scaled such that the total transmit energy is the same as when multiple rounds of the unimodular sequence is used. The results of the simulation are averaged over 50 trials and the transmit SNR is varied from -10dB to 10dB. It can be seen in Fig. 3 that at -10dB, there is a 42% decrease in error rate using the unimodular sequence. As the transmit SNR is increased, say at 10dB, the percentage error difference between the two transmit signal approaches becomes smaller. This implies that the proposed algorithm is effective, especially in noisy conditions which is typically the case in useful scenarios.

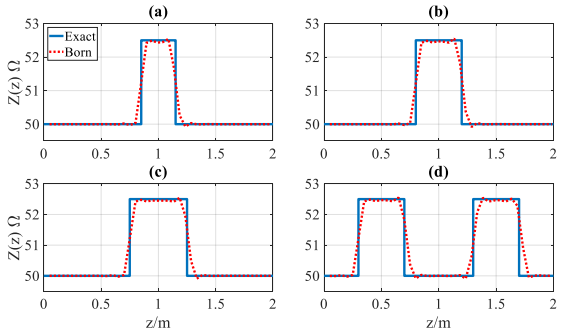

Fig. 2: Reconstruction of baseband case with different fault lengths: (a) 0.3m, (b) 0.4m, (c) 0.5m, (d) concatenated 0.4m fault.

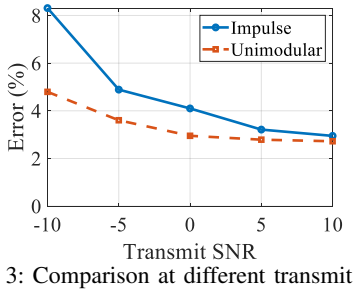

Fig. 3: Comparison at different transmit SNR

B. Passband Set-up

In this section, the effect of a bandlimited sequence in the reconstruction process is evaluated. The reconstructions are shown in Fig. 4, in which we can see varying results. It is interesting to note that a good reconstruction is made when the fault length is 0.5 m. However, this is coincidental as its channel frequency response is periodic at 4 GHz. For the rest of the fault lengths, reconstruction error starts to manifest itself after the downward edge of the rectangular profile. A similar trend can also be observed for a profile with two concatenated faults of 0.4m in Fig. 4(d).

We then implement the proposed method with sample accumulation and the results are shown in Fig. 5. Results demonstrate significant improvement compared to the standard passband case. The errors e_{rel} corresponding to Fig. 5 (a)-(d) are $5.5\%, 4.2\%, 4.7\%$, and 9.9% respectively, which are relatively close to the baseband results. This implies a successful reconstruction of the rectangular impedance profiles. Finally, the effect of noise in the reconstruction is considered and tested by adding white Gaussian noise to a channel with 0.4 m fault length. Results are shown where the transmit SNR for Fig. 6 (a)-(d) are 10dB, 3dB, -3dB, and -10dB, and its corresponding error e_{rel} are $6.6\%, 8.28\%, 10.0\%$, and 22.6% respectively. It can be noticed that reconstruction quality starts to be affected at -3dB and breaks down at -10dB. Overall, results suggest that the added procedure is able to estimate the entire channel and successfully reconstruct rectangular profiles.

The proposed approach with sample accumulation can work for any impedance profile with a sparse channel impulse response, such as the tested rectangular case. Obtaining experimental results is tthe next step that needs to be taken to verify the results in actual transmission line scenarios. Several factors that could affect the experimental set-up, such as non-linearities and local oscillator leakage, are left for future work.

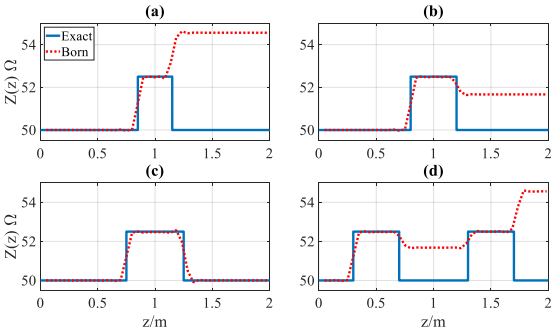

Fig. 4: Reconstruction of passband case with different fault lengths: (a) 0.3m, (b) 0.4m, (c) 0.5m, (d) concatenated 0.4m fault

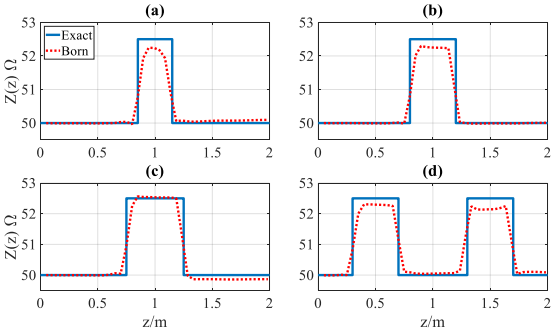

Fig. 5: Passband case with accumulation in different fault length: (a) 0.3m, (b) 0.4m, (c) 0.5m, (d) concatenated 0.4m fault

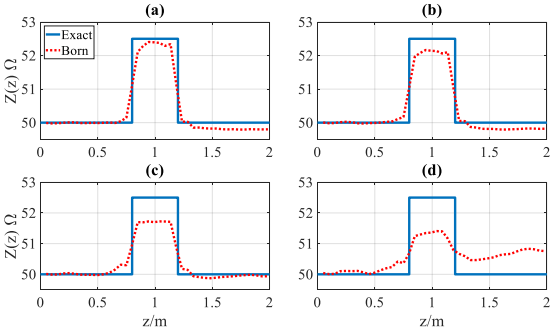

Fig. 6: Test on different transmit SNR: (a) 10dB, (b) 3dB, (c) -3dB, (d) -10dB

VI. Conclusion

We have demonstrated the use of bandlimited passband signals with adaptive sequence design to obtain reconstructions of impedance profiles. While the use of passband signals limits the channel information for reconstruction, rectangular profiles can be estimated effectively by compensating for the modulation and demodulation of the passband sequence using sample accumulation. This is possible since rectangular profiles have sparse channel impulse response. Overall results from the simulations have demonstrated that the proposed method performs well.

Acknowledgement

We would like to thank the Hong Kong Research Grants Council for their grant 16232316.

REFERENCES

[1] Y.-J. Shin, E. J. Powers, T.-S. Choe, C.-Y. Hong, E.-S. Song, J.-G. Yook, and J. B. Park, "Application of Time-Frequency Domain Reflectometry for Detection and Localization of a Fault on a Coaxial Cable," *IEEE Transactions on Instrumentation and Measurement*, vol. 54, no. 6, pp. 2493–2500, 2005.

[2] Q. Zhang, M. Sorine, and M. Admane, "Inverse Scattering for Soft Fault Diagnosis in Electric Transmission Lines," *IEEE Transactions on Antennas and Propagation*, vol. 59, no. 1, pp. 141–148, 2011.

[3] Y. Takamatsu, T. Seiyama, H. Takahashi, Y. Higami, and K. Yamazaki, "On the Fault Diagnosis in the Presence of Unknown Fault Models using Pass/Fail Information," in *2005 IEEE International Symposium on Circuits and Systems (ISCAS)*. IEEE, 2005, pp. 2987–2990.

[4] V. Fochi, E. Wächter, A. Erichsen, A. M. Amory, and F. G. Moraes, "An Integrated Method for Implementing Online Fault Detection in NoC-based MPSoCs," in *2015 IEEE International Symposium on Circuits and Systems (ISCAS)*. IEEE, 2015, pp. 1562–1565.

[5] A. M. Gharehbaghi and M. Fujita, "A New Approach for Diagnosing Bridging Faults in Logic Designs," in *2017 IEEE International Symposium on Circuits and Systems (ISCAS)*. IEEE, 2017, pp. 1–4.

[6] L. A. Griffiths, R. Parakh, C. Furse, and B. Baker, "The Invisible Fray: A Critical Analysis of the Use of Reflectometry for Fray Location," *IEEE Sensors Journal*, vol. 6, no. 3, pp. 697–706, 2006.

[7] W. Wang, L. Jing, Z. Li, and R. D. Murch, "Utilizing the Born and Rytov Inverse Scattering Approximations for Detecting Soft Faults in Lossless Transmission Lines," *IEEE Transactions on Antennas and Propagation*, vol. 65, no. 12, pp. 7233–7243, 2017.

[8] W. Wang, Y. Li, Z. Li, and R. Murch, "Super-resolution Results for a 1D Inverse Scattering Problem," in *ICASSP 2019-2019 IEEE International Conference on Acoustics, Speech and Signal Processing (ICASSP)*. IEEE, 2019, pp. 4240–4244.

[9] Z. Wang, P. Babu, and D. P. Palomar, "Design of PAR-Constrained Sequences for MIMO Channel Estimation via Majorization–Minimization," *IEEE Transactions on Signal Processing*, vol. 64, no. 23, pp. 6132–6144, 2016.

[10] W.-M. Boerner, "Electromagnetic Inverse Methods and its Applications to Medical Imaging - A Current State-of-the-Art Review," in *IEEE International Symposium on Circuits and Systems (ISCAS)*. IEEE, 1989, pp. 999–1006.

[11] N. Weng, Y.-H. Yang, and R. Pierson, "Three-dimensional Surface Reconstruction using Optical Flow for Medical Imaging," *IEEE Transactions on Medical Imaging*, vol. 16, no. 5, pp. 630–641, 1997.

[12] A. Khwaja and X.-P. Zhang, "Compressed Sensing SAR Moving Target Imaging in the Presence of Basis Mismatch," in *2013 IEEE International Symposium on Circuits and Systems (ISCAS)*. IEEE, 2013, pp. 1809–1812.

[13] F. Wang, T. F. Eibert, and Y.-Q. Jin, "Simulation of ISAR Imaging for a Space Target and Reconstruction under Sparse Sampling via Compressed Sensing," *IEEE Transactions on Geoscience and Remote Sensing*, vol. 53, no. 6, pp. 3432–3441, 2015.

[14] A. Shabat and V. Zakharov, "Exact Theory of Two-dimensional Self-focusing and One-dimensional Self-modulation of Waves in Nonlinear Media," *Soviet Physics JETP*, vol. 34, no. 1, p. 62, 1972.

[15] D. M. Pozar, *Microwave engineering*. John Wiley & Sons, 2009.